

## Development of 4D Monte Carlo Dose Calculation Program by Using Posture-deformed Mesh Phantoms and its Potential Application to Real-time Dose Monitoring System

Haegin Han<sup>a</sup>, Chansoo Choi<sup>a</sup>, Bangho Shin<sup>a</sup>, Yeon Soo Yeom<sup>b</sup>, Chan Hyeong Kim<sup>a\*</sup>

<sup>a</sup>Department of Nuclear Engineering, Hanyang University, 222 Wangsimni-ro, Seongdong-gu, Seoul 04763, Korea

<sup>b</sup>National Cancer Institute, National Institute of Health, 9609 Medical Center Drive, Bethesda, MD 20850, USA

\*Corresponding author: [chkim@hanyang.ac.kr](mailto:chkim@hanyang.ac.kr)

### 1. Introduction

Unlike in other medical procedures that involve radiations, medical staffs in image-guided interventional radiography procedures remain inside the imaging room, and for required cases, they even stay close to the patients, causing relatively high doses by scattered radiation [1]. Severe radiation injuries to interventional radiologists, especially in lens and skin, have been extensively reported by many literatures [2-6]. Occupational radiological protection issues in interventional procedures are recently being more highlighted with the increase in the number of interventions and their diversity and complexity.

In most cases for regular monitoring, the doses to medical staffs are evaluated by passive dosimeters, usually by TLD-type dosimeter, and in other limited cases for dose optimizations, active personal dosimeters are used, which can provide immediate alert for high dose rate and time variation of doses. However, both passive and active dosimeters cannot provide dose values for specific organs, and thus for more accurate estimations for organ absorbed and effective doses and for more precise dose optimizations, advanced computational dose calculations should be performed and the relations between the measured value and organ absorbed or effective doses should be investigated [1]. Regarding this, a real-time computational dose monitoring system was developed by Badal *et al.* [7], which calculated organ doses of a medical staff in real-time by continuously adjusting the position of the detailed human phantom from the Virtual Family [8] according to the data obtained from Kinect device. This system, however, used the phantom only in standing posture without considering the effects by posture.

To investigate of the influence of posture to dose values, various researchers have developed phantoms in different postures, mostly constructed by manually deforming voxel or boundary representation (BREP) phantoms [9-11]. Xu *et al.* [12] obtained rather realistic posture data from motion capture system and directly applied obtained data by replacing joint areas of BREP phantoms by spherical hinges. Very recently, Yeom *et al.* [13] developed phantoms in five different postures by deforming mesh-type reference computational phantoms (MRCPs), which are the most advanced form of computational phantoms for radiation dose calculations. Although there were some discrepancies in dose values, all these previous studies concluded that non-standing phantoms can yield significantly different dose values

from those for standing phantoms. While the doses for static postures were extensively investigated, the method to calculate doses for moving posture was not yet been developed.

In the present study, a Geant4-based 4D Monte Carlo dose calculation program was developed to automatically deform the posture of mesh phantom and directly calculate doses for the deformed phantom. The developed program was then used to calculate organ absorbed doses for dynamic posture data obtained from a motion capture system. In addition, feasibility study was conducted to investigate its potential application to real-time dose monitoring system.

### 2. Methods and Results

#### 2.1 Posture Deformation Methodology

In the present study, the adult male MRCP was first separated into organless body and internal organ phantoms. Then, the organless body phantom was slightly modified for mesh stabilization and the secure of enough space between bones in limb joint areas (i.e., shoulder, elbow, wrist, hip, knee, and ankle). Note that on-time posture deformation was performed only for organless body phantom, and the internal organ phantom was pre-deformed into various rotation angles and constructed as a database. This was because internal organ phantom requires much longer computational time for deformation due to their complexity and its relatively smaller rotation range than that of limb joints.

For the posture deformation of the organless body phantom, 13 joint regions (i.e., spine joint and limb joints for both sides) were first defined, and each joint was deformed in sequence according to the corresponding rotation matrix provided by motion capture data. The mesh in each region was deformed by using the technique based on volumetric graph Laplacian (VGL) [14] which alleviated unnatural volume changes and local self-intersections for large deformations.

The database for internal organ phantoms was constructed by deforming them according to the rotation of spine joint. For this, rotation matrices to cover the range of spine joint movement were first selected, and the internal organ phantom was deformed for the selected matrices by using as-rigid-as-possible (ARAP) algorithm [15] which can be better applied to the rather complicated meshes than the technique based on VGL. For each rotation matrix, the outer skin surface of organless body phantom, correspondingly deformed by the VGL

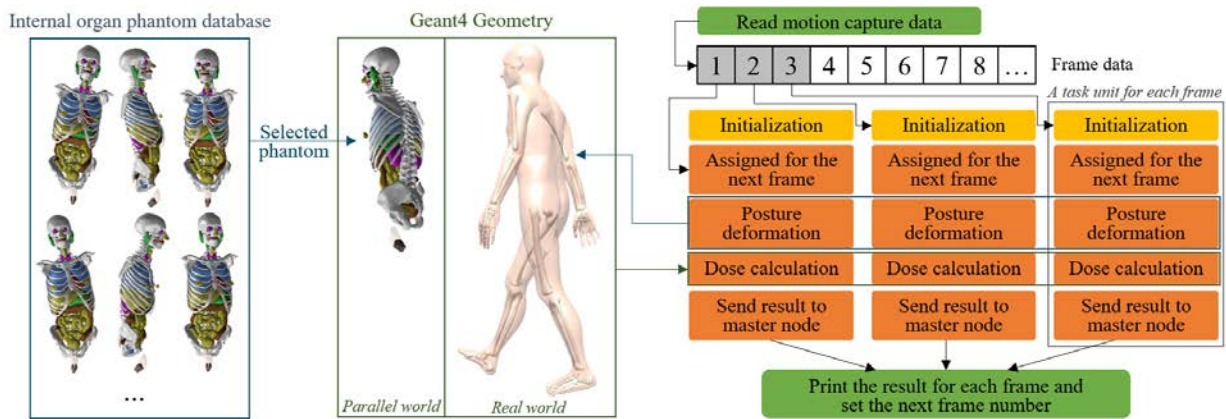


Fig. 1. Procedure flowchart for the 4D Monte Carlo simulation program for posture-changing mesh phantom developed in the present study.

technique, was also considered to prevent the exposure of internal organ phantoms.

## 2.2 Geant4-based 4D Monte Carlo Simulation Program

An integrated 4D Monte Carlo simulation program was developed by implementing a dedicated C++ program for posture deformation into Geant4 code, enabling it to calculate doses by directly using the deformed phantom data. Figure 1 is the flowchart that shows the overall procedure of the developed program. For dose calculations, the deformed organless body phantom was installed together with the internal organ model selected according to the rotation matrix of spine joint, by using the parallel world geometry feature of Geant4; that is, organless body phantom and internal organ phantom were implemented in *Real World* and *Parallel World*, respectively. The sequential tasks for each frame to deform the phantom and calculate the doses were parallelized by Intel® Message Passing Interface (MPI) library, so that one task after another for each frame can be assigned to each core at the end of the task for the previous frame. In addition, *G4Allocator* class was used to prevent the performance degradation due to the frequent allocation and deallocation of the large memory required for phantom data of each frame. For the verification, the developed program was used to calculate time variation of organ-averaged absorbed doses to 37 MBq  $^{60}\text{Co}$  point source by using the motion data file in Biovision Hierarchy (BVH) format obtained from motion capture system. The simulations were performed on 40 cores of the Intel® Xeon® CPU E5-2698 v4 (@ 2.20 GHz CPU processor and 256 GB RAM memory).

## 3. Result

Figure 2 shows the position of  $^{60}\text{Co}$  source and ten posture-deformed organless body phantoms among the 98 phantoms (frame time: 0.17 s). It can be seen that the phantoms were deformed in realistic appearance for both

walking and sitting motions. The volume loss by deformation was less than 3% for all the frames, and it was less than 0.2% when only walking frames (0-6.8 s) were considered.

Figure 3 shows the time variation of organ-averaged absorbed doses calculated in the present study, for colon, liver, brain, and lungs. It can be seen that the doses to all organs gradually increase as the phantom walks toward the source (0-6.8 s), and that they plateau while it turns around to sit (6.8-10.0 s). Then a sudden drop follows during a short period at which the source is blocked by the right hand (10.0-11.0 s), and finally the doses increase as the phantom sits (11.0-12.5 s) and plateaus after completion of sitting. It can also be seen that when the source is near the phantom (6.8-16.7 s), the organs near at the source level receive higher doses.

To develop real-time dose monitoring system by applying this 4D Monte Carlo simulation program, which is the ultimate goal of the current study, computational time should be most importantly considered. For the dose calculation performed in the present study, where  $10^6$  particles were transported for each frame, the computational time was 3.4 s per frame. This implies that real-time dose calculations may be possible only for the motions data with frame time longer than 3.4 s. However, as the computational time is inversely proportional to the number of the cores, it can be significantly decreased when an enough number of cores are secured, enabling real-time dose calculations for shorter frame times.

## 4. Conclusions

In the present study, a Geant4-based 4D Monte Carlo program was developed and its feasibility to be applied to the real-time dose monitoring system was investigated. The developed program was used to calculate time variation of organ-averaged absorbed doses by using posture data obtained from motion capture system. It was found that the developed program realistically deformed the mesh phantom into different postures and directly

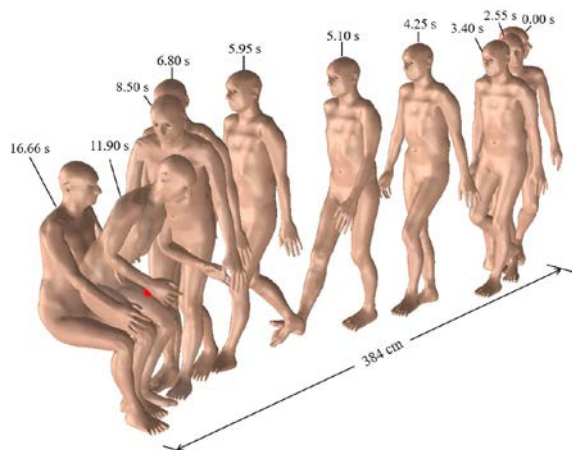


Fig. 2. Position of  $^{60}\text{Co}$  source (red spot) and organless body phantoms deformed by posture data obtained from motion capture system.

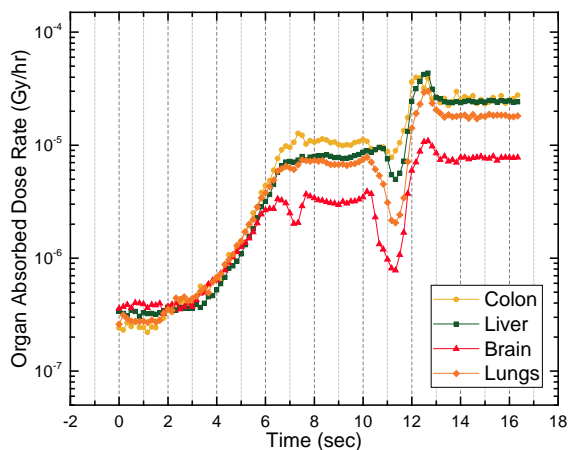


Fig. 3. Variation of organ-average absorbed dose as function of time for colon, liver, brain, and lungs, calculated by using the phantoms deformed into continuous postures by using the data from motion capture system.

calculated the organ-averaged absorbed doses by using the deformed phantoms. In this program, the task for each frame was parallelized by MPI library, and thus the computation speed can be further improved when a large number of cores are secured. The final goal of the present study is the development of real-time organ dose monitoring system, and for this, computational performance will be enhanced by utilizing a cluster server and on-time posture data input will be enabled by data streaming technique.

The developed program may be highly useful for various fields that requires dose monitoring or optimization, including not only radiological image-guided interventions, but also necessary high-dose radiation tasks (e.g., steam generator tube plugging task in pressurized water reactors (PWRs)). In addition, the program can be used for the precise establishment of dose conversion factors for dosimeters by time-by-time

comparison between the values measured in dosimeters and calculated absorbed organ doses, or also can be used for dose reconstructions for accidental exposures.

## REFERENCES

- [1] ICRP, Occupational Radiological Protection in Interventional Procedures, ICRP Publication 139, Ann. ICRP 47(2), 2018.
- [2] A. K. Junk, Z. Hakal, and B. V. Worgul, Cataract in interventional radiology-an occupational hazard?, *Investigative Ophthalmology & Visual Science* 45(13), pp. 338, 2004.
- [3] T. B. Shope, Radiation-induced skin injuries from fluoroscopy, *Radiographics* 16(6), pp. 1195-1199, 1996.
- [4] D. L. Miller, S. Balter, P. E. Cole, H. T. Lu, *et al.*, Radiation doses in international radiology procedures: the RAD-IR study. Part I: overall measures of dose, *Journal of vascular and interventional radiology* 14(6), pp. 711-727, 2003.
- [5] D. L. Miller, S. Balter, P. E. Cole, H. T. Lu, *et al.*, Radiation doses in international radiology procedures: the RAD-IR study. Part II: skin dose, *Journal of vascular and interventional radiology* 14(8), pp. 977-990, 2003.
- [6] S. Balter, J. W. Hopewell, D. L. Miller, *et al.*, Fluoroscopically guided interventional procedures: a review of radiation effects on patients' skin and hair, *Radiology* 254(2), pp. 326-341, 2010.
- [7] A. Badal, F. Zafar, H. Dong, and A. Badano, A real-time radiation dose monitoring system for patients and staff during interventional fluoroscopy using GPU-accelerated Monte Carlo simulator and an automatic 3D localization system based on a depth camera, *proceedings of SPIE*, 2013.
- [8] A. Christ, W. Kainz, E. G. Hahn, *et al.*, The Virtual Family-development of surface-based anatomical models of two adults and two children for dosimetric simulations, *Physics in Medicine & Biology* 55(2), N23-N38, 2010.
- [9] L. Su, B. Han, and X. G. Xu, Calculated organ equivalent doses for individuals in a sitting posture above a contaminated ground and a PET imaging room, *Radiation protection dosimetry* 148(4), pp. 439-443, 2011
- [10] F. R. Cavalcante, D. C. Galeano, A. B. Carvalho Junior, *et al.*, Comparison of conversion coefficients for equivalent dose in terms of air kerma using a sitting and standing female adult voxel simulators exposure to photons in antero-posterior irradiation geometry. *Radiation Physics and Chemistry* 95, pp. 158-160, 2014.
- [11] D. C. Galeano, W. S. Santos, M. C. Alves, *et al.*, Fluence-to-dose conversion coefficients based on the posture modification of Adult Male (AM) and Adult Female (AF) reference phantoms of ICRP 110, *Radiation Physics and Chemistry*, 121, pp. 50-60, 2016.
- [12] J. A. Vazquez, P. F. Caracappa, and X. G. Xu, Development of posture-specific computational phantoms using motion capture technology and application to radiation dose-reconstruction for the 1999 Tokai-Mura nuclear criticality accident, *Physics in Medicine & Biology* 59(18), pp. 5277, 2014.
- [13] Y. S. Yeom, H. Han, C. Choi, *et al.*, I. posture-dependent dose coefficients of mesh-type reference computational phantoms for photon external exposures, *Health Physics*, in press.
- [14] K. Zhou, J. Huang, J. Snyder, *et al.*, Large mesh deformation using the volumetric graph Laplacian, *ACM transactions on graphics (TOG)*, pp. 496-503, 2005.
- [15] H. B. Yan, S. Hu, R. R. Martin, *et al.*, Shape deformation using a skeleton to drive simplex transformations. *IEEE*

Transactions on Visualization and Computer Graphics, 14(3),  
pp.693-706, 2008.